Supporting Information

Bar-Oz et al. 10.1073/pnas.1017647108

SI Materials and Methods

Context of Faunal Material. Tell Kuran is a typical Near Eastern tell (i.e., mounded site) composed on the degraded remains of unfired mud brick buildings and refuse deposits. The site, on the right bank of the Khabur River, has lost much of its mass through riverside erosion. A number of ashy deposits from the eroded riverside slope were sampled, one of which yielded the bone deposit. Excavation of an area of some 2 m^2 over a depth of 10–15 cm revealed a compact mass of gazelle bones. This deposit lay on a compact, essentially flat surface and was sealed above by a layer of mud bricks of a subsequent phase of building construction, which occurred, according to the condition of the bones, shortly after the bones were deposited. No attempt was made to dig beyond the small area indicated, and it is possible that further evidence of the deposit lies within the mound. It is probable that much of the deposit had eroded down the slope and into the river. During excavation, it became clear that this was a unique deposit. Typically, archaeological middens that accumulate as a result of intermittent deposition of refuse contain a mix of faunal species and body parts along with bits of pottery, stone tools, plant material, ash, and construction debris; however, the Kuran E deposit held nothing but bones. The date of the Kuran E deposit was established by tracing the stratum for some meters horizontally to where it contained both diagnostic ceramics and charred material, which was radiocarbon-dated.

Zooarchaeological Procedures. The bone deposit of Area E at Tell Kuran was analyzed meticulously and systematically. All identifiable bone fragments were studied. Identified specimens whose precise location in the skeletal element or portion could be determined and quantified (i.e., NISP) were recorded according to skeletal element. These included cranial elements, vertebrae, long bone articular ends and shafts, and all recognizable bone and teeth. Identified specimens were also coded according to their fraction of completeness (i.e., percentage of the portion of the element represented). This procedure allowed us to compute the minimum number of skeletal elements (MNE), the minimum animal units (MAU), and the minimum number of individuals, as described previously (1, 2). Anatomical measurements were obtained as described previously (3).

Each recorded specimen was examined under a 10× Nikon stereomicroscope with an oblique light source for bone surface modifications induced by humans (butchery, burning, and fracturing), animals (principally carnivore puncture, scoring, and digestion) and other agents (weathering, trampling, and root activity) (2, 4–7). Data were obtained from the literature for bone mineral density data in *Rangifer tarandus* (8), for the Food Utility Index in *R. tarandus* (9), and for marrow values in *G. gazella* (10).

In addition, a sample of limb shaft fragments was analyzed to explore whether bones were broken fresh (green) or old (dry). Fractures with recent breakage caused during extraction or handling were excluded. The morphology of the fracture angle and fracture outline was recorded as described previously (11).

The age and sex structure of the gazelle population was analyzed using tooth wear and epiphyseal closure data, with tooth wear and epiphyseal fusion stages determined as described previously (12). Frequencies of male and female gazelles were calculated using second phalanx measurements and horn and scapula morphology, as described previously (13).

1. Klein RG, Cruz-Uribe K (1984) *The Analysis of Animal Bones From Archaeological Sites* (Chicago Univ Press, Chicago).
2. Lyman LR (1994) *Vertebrate Taphonomy* (Cambridge Univ Press, Cambridge, U.K.).
3. Driesch AVD (1976) *A Guide to a Measurement of Animal Bones From Archaeological Sites* (Peabody Museum Press, Cambridge, MA).
4. Behrensmeyer AK (1978) Taphonomic and ecological information from bone weathering. *Paleobiology* 4:150–162.
5. Behrensmeyer AK, Gordon KD, Yanagi GT (1986) Trampling as a cause of bone surface damage and pseudo-cutmarks. *J Anthropol Archaeol* 25:436–447.
6. Binford L (1981) *Bones: Ancient Men and Modern Myths* (Academic, New York).
7. Blumenschine RJ, Marean CW, Capaldo SD (1996) Blind tests of inter-analyst correspondence and accuracy in the identification of cut marks, percussion marks, and carnivore tooth marks on bone surfaces. *J Archaeol Sci* 23:493–507.
8. Lam YM, Chen X, Pearson OM (1999) Intertaxonomic variability in patterns of bone density and the differential representation of bovid, cervid, and equid elements in the archaeological record. *Am Antiq* 64:343–362.
9. Metcalfe D, Jones KT (1988) A reconsideration of animal body part utility indices. *Am Antiq* 53:486–504.
10. Bar-Oz G, Munro ND (2007) Gazelle bone marrow yields and Epipalaeolithic carcass exploitation strategies in the southern Levant. *J Archaeol Sci* 34:946–956.
11. Villa P, Mahieu E (1991) Breakage patterns of human long bones. *J Hum Evol* 21: 27–48.
12. Munro ND, Bar-Oz G, Stutz AJ (2009) Aging mountain gazelle: Refining methods of tooth eruption and wear and bone fusion. *J Archaeol Sci* 36:752–763.
13. Munro ND, Bar-Oz G, Hill AC (2011) Exploration of character traits and linear measurements for sexing mountain gazelle (*Gazella gazella*) skeletons. *J Archaeol Sci*, in press.
14. Eschallier J, Braemer F (1995) Nature et functions des "desert kites," données et hypotheses. *Paléorient* 21:35–63.
15. Lyman LR (1987) On the analysis of vertebrate mortality profiles: Sample size, mortality type, and hunting pressure. *Am Antiq* 52:125–142.
16. Stiner MC (1990) The use of mortality patterns in archaeological studies of hominid predatory adaptations. *J Anthropol Archaeol* 9:305–351.

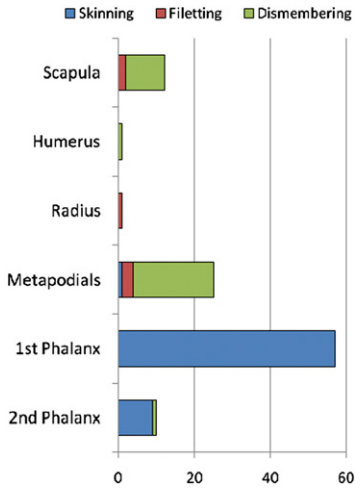

Fig. S1. Number of gazelle bones (NISP) with butchery marks and activities with which they might be associated.

Fig. S2. Butchery scars on gazelle first phalanges. All phalanges are shown in the anterior view (photo credit: Adam S. Watson).

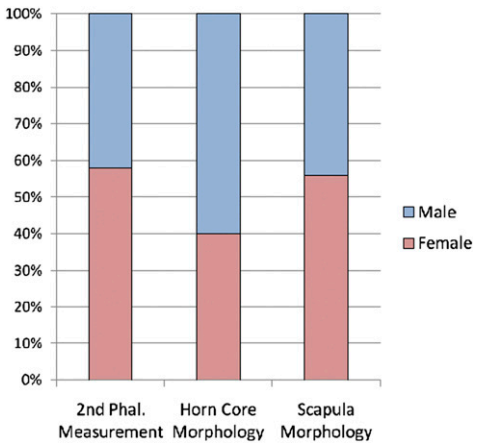

Fig. S3. Sex distribution of second phalanges length, horn core morphology, and scapula morphology in Kuran E gazelle.

Table S1. Faunal assemblages from the Khabur Basin

Region	Period	Dates cal BCE	Site name	Site	Domestic	Gazelle	Equus	Other wild	Total NISP
North	PPN/PN	7000–6500	Feyda	K124	78.1%	13.8%	0.0%	8.2%	196
	Ceramic Neolithic	6700–6200	Tell Halaf	K137	9.1%	54.5%	0.0%	36.4%	11
	Proto-Hassuna	5800–5500	Kashkashok II	K119	76.9%	23.1%	0.0%	0.0%	13
	Late Halaf	5800–5500	Kashkashok I	K120	93.2%	4.4%	0.3%	2.1%	385
	Post-Ubaid	4900–4500	Kuran D	K125	39.2%	52.9%	3.9%	3.9%	51
	Post-Ubaid	4500–4300	Tell Brak	K132	64.7%	0.0%	5.9%	29.4%	17
	Early Uruk	3900–3600	Kashkashok I	K120	97.8	0	0	2.2%	45
	Late Uruk	3600–3100	Kuran E	K125-E	0.6%	99.3%	0.1%	0	2649
	Late Uruk	3600–3100	Kuran F	K125-F	61.6%	15.5%	2.8%	20.1%	284
	Mid III	3000–2800	Leilan IIIb		93.4%	1.3%	3.0%	2.4%	6382
	Nuzi	2000–1800	Kashkashok IV	K121	91.6%	4.8%	3.6%	0.0%	166
South	Halafian	5900–5500	Umm Qseir	K138	30.9%	54.9%	11.1%	3.1%	3511
	Ubaid	5200–4500	Ziyadeh	K115	48.6%	19.8%	26.5%	5.1%	2671
	Ubaid	5200–4900	Mashnaqqa	K116	13.9%	29.3%	21.3%	35.4%	811
	Post-Ubaid	4500–4000	Ziyadeh	K115	42.6%	21.0%	29.2%	7.2%	2315
	Post-Ubaid	4500–4300	Mashnaqqa	K116	63.8%	9.1%	25.0%	2.1%	679
	Uruk	3900–3600	Umm Qseir	K138	29.6%	44.3%	24.7%	1.4%	636
	Uruk	3900–3500	Mashnaqqa	K116	75.0%	20.0%	5.0%	0.0%	20
	Ninevite 5	3300–2600	Ziyadeh	K115	44.1%	40.1%	3.3%	12.5%	152
	Ninevite 5	3000–2500	Atij		66.2%	14.9%	17.3%	1.6%	1853
	Ninevite 5	3000–2500	Raqai		81.2%	11.0%	3.6%	4.2%	3131
	Ninevite 5	3000–2500	Gudeda		84.8%	3.5%	3.5%	8.2%	682
	Ninevite 5	3000–2500	Mashnaqqa	K116	89.4%	6.4%	4.3%	0.0%	78

Table S2. Kuran E gazelle skeletal element frequency

	NISP	MNE	MNI	%MAU
Head				
Horn	7	5	3	3.2%
Occipital condyle	4	4	2	2.2%
Petrosum	11	11	6	6.5%
Maxilla	3	3	3	3.2%
Total skull fragments	25	11	6	6.5%
Mandible fragments	43	32	16	17.2%
Mandible ramus condyle	18	18	9	9.7%
Total mandible fragments	61	32	16	17.2%
Isolated mandible teeth	12	12	2	
Isolated maxilla teeth	13	13	2	
Body				
Axis	1	1	1	1.1%
Cervical vertebrae	1	1	1	1.1%
Thoracic vertebrae	4	3	1	1.1%
Lumbar vertebrae	7	6	1	1.1%
Rib, head	8	8	1	1.1%
Rib, medial shaft	16	6	1	1.1%
Rib, total	31	8	1	1.1%
Forelimb				
Scapula, glenoid fossa	80	78	43	46.2%
Scapula, shoulder blade	78	14	7	7.5%
Scapula, total	158	78	43	46.2%
Humerus, proximal	6	4	2	2.2%
Humerus, medial shaft	8	3	2	2.2%
Humerus, distal	8	8	4	4.3%
Humerus, total	22	8	4	4.3%
Radius, proximal	4	4	2	2.2%
Radius, medial shaft	6	3	2	2.2%
Radius, distal	7	7	6	6.5%
Radius, total	17	7	6	6.5%
Ulna, complete	5	5	3	3.2%
Ulna, proximal	2	1	1	1.1%
Ulna, total	7	5	3	3.2%
Metacarpus, proximal	6	3	2	2.2%
Metacarpus, medial shaft	2	1	1	1.1%
Metacarpus, distal	9	8	4	4.3%
Metacarpus, total	17	8	4	4.3%
Hindlimb				
Pelvic acetabulum, complete	2	2	1	1.1%
Pelvic acetabulum, illium	3	3	2	2.2%
Pelvic ilium, caudal	2	2	1	1.1%
Pelvic acetabulum, ischium	2	2	2	2.2%
Pelvic acetabulum, pubis	4	3	2	2.2%
Pelvic, total	13	5	3	3.2%
Femur, complete	1	1	1	1.1%
Femur, proximal	18	12	6	6.5%
Femur, medial shaft	5	2	1	1.1%
Femur, distal	7	6	3	3.2%
Femur, total	31	13	7	7.5%
Tibia, proximal	3	3	2	2.2%
Tibia, distal	8	6	3	3.2%
Tibia, total	11	6	3	3.2%
Astragalus	3	3	2	2.2%
Calcaneus, complete	2	2	1	1.1%
Metatarsus, complete	1	1	1	1.1%
Metatarsus, proximal	9	7	4	4.3%
Metatarsus, medial shaft	3	1	1	1.1%
Metatarsus, distal	13	11	6	6.5%
Metatarsus, total	26	12	7	7.5%
Toes				
Phalanx 1, complete	511	510	64	68.8%
Phalanx 1, proximal	124	112	14	15.1%

Table S2. Cont.

	NISP	MNE	MNI	%MAU
Phalanx 1, distal	244	228	29	31.2%
Phalanx 1, total	879	738	93	100.0%
Phalanx 2, complete	519	519	65	69.9%
Phalanx 2, proximal	27	26	4	4.3%
Phalanx 2, distal	78	76	10	10.8%
Phalanx 2, total	624	595	75	80.6%
Phalanx 3, proximal	2	2	1	1.1%
Phalanx 3, complete	519	513	65	69.9%
Phalanx 3, total	521	515	66	71.0%
Metapod, condyle	147	146	19	20.4%
Metapod, medial shaft	5	3	2	2.2%
Metapod, total	152	146	19	20.4%
Total	2,631	2,077	93	

MNI, minimum number of individuals.

Table S3. Summary of key taphonomic variables for Kuran E gazelle

Density-mediated attrition	
Correlation, bone mineral density vs. %MAU	MAU = 0.246(BMD) − 0.014
Spearman's *r*	0.196
P value	0.30
Proximal/distal humerus MNE	4/8
Proximal/distal tibia MNE	3/6
% Astragals complete	3/3
Total NISP/MNE	1.28
Bone surface modification	
% Trampling*	1.9%
% Root marks*	2.5%
% Weathering (≥ stage 3)*	3.2%
% Carnivore gnaw*	9.7%
% Rodent gnaw*	0.0%
% Cut-marked bones	4.0%
% Percussion marks*	0.5%
% Long-bone green fractures*	78.4%
% Burned	0.2%
Correlation, Food Utility Index (FUI) vs. %MAU	MAU = −0.0018(FUI) + 0.024
Spearman's *r*	0.21
P value	0.47
Correlation, Marrow Index vs. NISP/MNE	Marrow Index = 13.303(NISP/MNE) − 0.6354
Spearman's *r*	0.48
P value	0.23

*Of total long-bone ends and mandible fragments (NISP = 370).

Table S4. Frequency of butchery marks on gazelle bones and activities with which they may be associated

Element	NISP	Code	Function
Scapula, glenoid cavity	6	S-1	Dismemberment
Scapula, glenoid cavity	4	S-2	Dismemberment
Scapula, shoulder blade	2	S-3	Filleting
Humerus, distal	1	Hd-2	Dismemberment
Radius, proximal	1	Rcp-6	Filleting
Metatarsus, distal	1	Mtd-2	Skinning
Metatarsus, distal	2	Mtd-1	Dismemberment
Metapod, condyle	13	Mp-1	Dismemberment
Metapod, condyle	8	Mp-3	Dismemberment
Metapod, condyle	3	Mp-4	Filleting
Phalanx 1	57	—	Skinning
Phalanx 2	9	—	Skinning
Phalanx 2	1	—	Hack
Total	108		

Butchering mark codes are equivalent to Binford's butchery mark typology (6).

Table S5. Tooth eruption and wear stages of complete mandibles of Persian gazelle in the Kuran E assemblage

Catalog no.	M3	M2	M1	P4	DP4	Age, months
1649	E	E	2	E	8	3
1651	E	E	2	E	7	3
1659	L	L	2	0	6	3
1642	E	E	5	E	11	3–7
1653	L	L	L	0	13	3–7
1658	L	L	L	L	9	3–7
1633	2	5	L	L	L	7–18
1634	1	3	6	1	—	7–18
1635	1	3	L	L	L	7–18
1645	2	7	L	L	L	7–18
1654	2	6	X	L	L	7–18
1656	2	X	X	L	L	7–18
1637	6	10	12	3	—	18–36
1638	6	10	12	2	—	18–36
1639	5	8	10	2	—	18–36
1640	7	10	12	X	—	18–36
1641	X	10	12	3	—	18–36
1643	6	8	X	X	L	18–36
1646	4	7	8	1	—	18–36
1632	9	10	L	L	—	36–54
1636	9	11	14	4	—	36–54
1647	9	10	L	X	—	36–54
1652	9	X	L	L	—	36–54
1644	10	12	13	4	—	54–96
1650	10	12	13	L	—	54–96
1655	L	L	14	4	—	54–96
1648	11	L	L	L	—	96+
1657	12	X	L	L	—	96+
1660	12	X	L	L	L	96+

The codes for each wear stage are given for dP4, P4, M1, M2, and M3. (X are teeth with broken cusps, E are teeth still erupting, and L are lost or missing teeth.) Tooth eruption and wear codes follow ref. 12 and Fig. 1.

Table S6. Ratio of unfused (UF) bones of gazelle in the Kuran E assemblage

	Fusion age, months	Neonatal	UF	Fusing	Fused	Total	%UF
Radius, proximal	3–7	0	0	0	4	4	
Phalanx 2, proximal		0	52	133	356	541	
Phalanx 1, proximal		0	211	26	391	628	
Humerus, distal		0	0	3	3	6	
Scapula, glenoid cavity		0	0	8	68	76	21.0
Tibia, distal	7–18	0	3	1	4	8	
Femur, proximal		0	9	1	5	15	
Calcaneum, proximal		0	1	0	1	2	
Metapod, distal		0	117	5	39	161	
Femur, distal		0	4	1	3	8	
Ulna, proximal		0	2	0	5	7	67.7
Humerus, proximal	18+	0	4	1	1	6	
Radius, distal		0	3	1	2	6	
Tibia, proximal		0	0	0	3	3	46.7

Fusion age data are from ref. 14.

Table S7. Kuran gazelle mortality profile divided into three age classes (young, prime-age adult, and old adult) compared with a theoretical living structure model and a catastrophic profile from St. Helens (15, 16)

	Young	Prime-age adult	Old adult	Total
Kuran gazelle	12 (42%)	14 (48%)	3 (10%)	29
Catastrophic profile in St. Helens	33 (38%)	49 (57%)	4 (5%)	86
Theoretical living structure model	19 (34%)	25 (45%)	11 (21%)	55

Table S8. Results of χ^2 comparisons between the Kuran gazelle mortality profile and case studies in Table S7

	N1	N2	df	χ^2	*P*
Kuran vs. catastrophic profile in St. Helens	29	86	3	1.34	0.72
Kuran vs. theoretical living structure model	29	55	3	1.58	0.66

Table S9. Frequency of male vs. female gazelles calculated using different metric and morphological methods

Method	Female	Male	Total
Second phalanx measurements	58%	42%	501
Horn morphology	40%	60%	5
Scapula morphology	56%	44%	41

Computational procedures are from ref. 13.